# Applications of cluster computing for the Anderson model of localization

Philipp Cain Frank Milde Rudolf A. Römer
Michael Schreiber
*Institut für Physik, Technische Universität, D-09107 Chemnitz, Germany*

**Abstract**

We consider parallelization strategies for the two most important algorithms used in numerical investigations of the Anderson model of localization, a paradigmatic model of disordered quantum systems. After a brief review of the physics of Anderson localization, we outline the Cullum-Willoughby implementation of the Lanczos diagonalization scheme and the transfer-matrix method used for the numerical characterization of localization properties. For applications of these algorithms to massively parallel cluster architectures, we develop and test various parallelization strategies.

*Key words:* Localization, Lanczos diagonalization, sparse matrices, parallelization
*PACS:* 71.23.k, 71.30.+h, 02.70.Hm

## 1. Introduction

Disordered systems represent a major challenge for modern computational methods. Due to their ubiquitous nature and their many applications, there is an ever growing need to understand the physics that governs their behavior [1–3]. Unfortunately, it is exactly their disordered nature that also makes any analytical approach and thus a simple mathematically tractable solution so very hard to come by. Nevertheless, in recent years a vast and extensive body of knowledge has been collected mainly based on extensive use of high-performance computing [2]. In the present paper, we will consider modern numerical approaches to the so-called Anderson model of localization [4], a quantum system of disordered electrons. In particular, we will review two recent efforts in constructing algorithms that work on modern day computer systems using scalable distributed memory and cluster architectures [5].

The paper is organized as follows. In section 2 we describe the underlying quantum physics problem, *i.e.*, the Anderson model of localization, and introduce the parameters used in our paper. In section 3 we briefly review the two main algorithms considered, namely the Cullum-Willoughby version of the Lanczos method and the transfer-matrix method. We then give in section 4 a detailed account of our parallelization strategies. We conclude in section 5.

## 2. The Anderson model of localization and its physics

The Anderson model of localization [4] is a paradigmatic model for the investigation of electronic properties of disordered systems [1–3]. Although it represents a severe simplification of amorphous materials [6], alloys [7,8], and disordered semiconductors [9,10], it is currently widely used in the theoretical description of quantum mechanical effects such as localization of electronic wave functions [11–15] and the metal-insulator transition (MIT) [16–18]. The quantum mechanical problem is represented mathematically by a Hamilton operator in the form of a real symmetric matrix $\mathbf{A}$. The quantum mechanical energy levels are given by the eigenvalues $E_n$ and the respective wave functions are simply the eigenvectors $\mathbf{x}_n$ of $\mathbf{A}$ [5]. *E.g.*, for a simple cubic lattice with $N \times N \times N$ sites, we have to solve the eigenvalue equation $\mathbf{A}\mathbf{x} = E\mathbf{x}$, which is given in site representation as

$$\begin{aligned} x_{i-1,j,k} + x_{i+1,j,k} + x_{i,j-1,k} + x_{i,j+1,k} + \\ x_{i,j,k-1} + x_{i,j,k+1} + \varepsilon_{i,j,k} x_{i,j,k} \\ = E x_{i,j,k}, \end{aligned} \tag{1}$$

with $i, j, k$ denoting the Cartesian coordinates of a site. The off-diagonal entries of $\mathbf{A}$ correspond to hopping amplitudes of the electrons from one site to a neighboring site and are chosen to be equal for simplicity. They have been set to one in (1) defining the energy scale. The disorder is encoded in the random potential site energies $\varepsilon_{i,j,k}$ on the diagonal of the matrix $\mathbf{A}$. We consider only the standard case of $\varepsilon_{i,j,k}$ being uniformly distributed in the interval $[-W/2, +W/2]$ with $W$ ranging from 1 to 30. The boundary conditions are usually periodic, but hard wall and helical [19] boundary conditions are sometimes also used. According to the Gersgorin circle theorem [20] every such matrix $\mathbf{A}$ has eigenvalues in the interval $[-W/2 - 6, +W/2 + 6]$. Possible generalizations of the Anderson model include anisotropic [21–26] or even random hopping [12–15], various choices of the distribution function of the site energies [27], a finite magnetic field [28–32] and spin effects [33–35].

Although the above matrix seems to be fairly simple, the intrinsic physics is surprisingly rich [1–3,36]. For small disorder ($W \ll 16.5$) and energies in the band centre ($|E| \ll 6$), the eigenvectors are extended, *i.e.*, $x_{i,j,k}$ is fluctuating from site to site but the envelope $|x|$ is approximately a non-zero constant. For large disorder ($W \gg 16.5$) and large energies ($|E| \gg 6$), all eigenvectors are localized, *i.e.*, the envelope $|x_n|$ of the $n$th eigenstate may be approximately written as $\exp[-|\mathbf{r} - \mathbf{r}_n|/\lambda_n(W)]$ with $\mathbf{r} = (i, j, k)^T$ and $\lambda_n(W)$ denoting the localization length of the eigenstate at the specified strength $W$ of the disorder [2]. $r_n$ denotes the approximate center of the eigenstate.

Since extended at temperature $T = 0$ states can contribute to electron transport, whereas localized states cannot, the Anderson model thus describes a $T = 0$ metal-to-insulator transition [2,3]: In three-dimensional samples for small disorder only few states in the band tails are localized. With increasing disorder more and more states became localized until at $W = W_c \approx 16.5$, the last remaining extended states at energy $E = 0$ vanish and no current can flow. Directly at $W_c$ there is a so-called critical regime where the eigenvectors are multifractal entities [19,23,27,37] showing characteristic fluctuations of the amplitude on all length scales, see Fig. 1. In order to numerically distinguish these three regimes, namely localized, critical and extended behavior, one needs to (i) go to extremely large system sizes and (ii) average over many different realizations of the disorder, *i.e.*, compute eigenvalues or -vectors for many matrices with different diagonals [38].

## 3. Numerical approaches to the problem

For the numerical characterization of the Anderson localization problem, we need to compute suitably chosen states and energies of the Hamilton matrix $\mathbf{A}$ of the Anderson model. Measures of localization can then be computed from multifractal analysis [19,23], energy level statistics [25,39–44], studies of participation numbers [12,13] and wave function statistics [45–50]. Therefore the computational task is to compute (a few) interior eigenvalues and the associated eigenvectors of a family

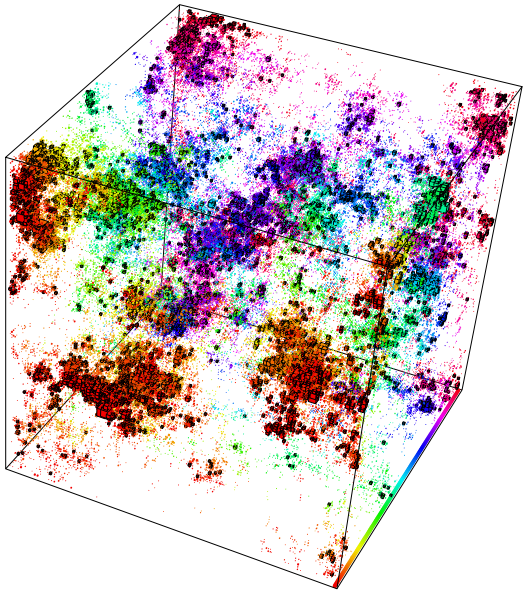

Fig. 1. Spatial probability distribution of a multifractal wave function at the Anderson transition ($W_c = 16.5$, $E = 0$) for an isotropic system of size $N^3 = 111^3 = 1367631$. Probability values larger than average are denoted by boxes of different sizes according to their value. Note how the wave function appears both extended throughout the whole system and at the same time localized to a few regions in space. The color code denotes the position with respect to the right bottom axis.

of structured large, sparse, real, symmetric, indefinite matrices.

### 3.1. *Solving the eigenvalue problem by Lanczos diagonalization*

Previously this problem was often solved by using the 1987 Cullum and Willoughby implementation of the Lanczos algorithm [51,52], in the following called CWI. This algorithm iteratively generates a sequence of orthogonal vectors $\mathbf{v}_i$, $i = 1, \ldots, K$, such that $\mathbf{V}_K^T \mathbf{A} \mathbf{V}_K = \mathbf{T}_K$, with $\mathbf{V} = \{\mathbf{v}_1, \mathbf{v}_2, \cdots, \mathbf{v}_K\}$ and $\mathbf{T}_K$ a symmetric tridiagonal $K \times K$ matrix. One obtains the recursion

$$\beta_{k+1} \mathbf{v}_{k+1} = \mathbf{A} \mathbf{v}_k - \alpha_k \mathbf{v}_k - \beta_k \mathbf{v}_{k-1}, \qquad (2)$$

where $\alpha_k = \mathbf{v}_k^T \mathbf{A} \mathbf{v}_k$ and $\beta_{k+1} = \mathbf{v}_{k+1} \mathbf{A} \mathbf{v}_k$ are the diagonal and subdiagonal entries of $\mathbf{T}_K$, $\mathbf{v}_0 = \mathbf{0}$ and $\mathbf{v}_1$ is an arbitrary starting vector. In finite precision arithmetic, the Lanczos vectors $\mathbf{v}_k$ typically lose their orthogonality after a small number of Lanczos iterations. Consequently, there usually appear so-called "spurious" or "ghost" eigenvalues in the spectrum $\sigma(\mathbf{T}_K)$, which do not belong to $\sigma(\mathbf{A})$. The solution to this problem as implemented in CWI [52] uses a simple and highly successful procedure to identify the spurious eigenvalues, thereby avoiding reorthogonalization.

In the last 10 years several new eigenvalue methods have been developed and implemented as software packages, that seem, at least at first glance, more

appropriate than CWI, see, *e.g.*, the recent survey and comparison given in Ref. [53]. In Ref. [5] we have tested several of these more modern methods to compute a few interior eigenvectors of the Anderson matrix. The implicitly restarted Arnoldi method [54] in connection with polynomial convergence acceleration [55] and in shift-and-invert mode with several direct and iterative solvers for the arising systems of linear equations [56] was compared to the CWI of the Lanczos method [51,52]. Despite the recent progress in linear system solvers [53] we found [5] all considered modern methods to be inapplicable for very large system sizes, because either the computation times or the memory requirements are much to large. Thus CWI Lanczos is currently still the most efficient method for the matrix type we are interested in and should therefore serve as the starting point for parallelization schemes. We emphasize that the wave function displayed in Fig. 1 is currently the largest such wave function ever to have been constructed [57].

### 3.2. *Solving the localization problem by transfer-matrix methods*

An alternative state-of-the-art method for computing localization lengths $\lambda$ directly is the so-called transfer-matrix method (TMM) [2,58–61]. This iterative method is very similar to the standard power series method for computing the largest eigenvalue [62]. It is based on rewriting the eigenvalue equation (1) in the recursion from

$$\mathbf{X}_{k+1} = (E\mathbf{I} - \mathbf{A}_k)\mathbf{X}_k - \mathbf{X}_{k-1} \qquad (3)$$

where $\mathbf{X}_k$ and $\mathbf{A}_k$ denote a complete set of wave vectors and the system matrix projected onto the $l$th slice of a quasi one-dimensional bar of length $L \gg M$, respectively. Here, $M$ indicates the transverse extent of the bar. Starting from a complete orthogonal basis set $\mathbf{X}_0$, *i.e.* a matrix with $2M^2 \times 2M^2$ entries, one can determine the Lyapunov exponents describing the exponential increase of the amplitudes along the bar. The inverse of the smallest exponent yields the physically relevant largest localization length $\lambda$.

There are two main benefits when using the TMM. First, it is not necessary to compute all wave functions. Since the system size to be considered should be at least of the same order as $\lambda$, this would be extremely memory and computation time consuming close to the MIT. Second, the accuracy can be controlled a priori in a TMM calculation due to the physics concept of self-averaging [2,59]. Thus there is no need for any a posteriori averaging over a large number of eigenstates. However, a major drawback of the method is an inherent instability due to loss of orthogonality of the initially complete basis set of vectors $\mathbf{X}_0$ onto which $\mathbf{A}$ is repeatetly multiplied. This instability due to finite precision arithmetic must be compensated by regularly applying a Gram-Schmidt reorthonormalization procedure [59].

## 4. Parallelization

Even when using well adapted numerical algorithms on state-of-the-art conventional single processor machines, the size of the system that can be treated is limited. This is a severe limitation, especially when critical properties close to an MIT are to be considered. Possible further progress can be achieved by using massively parallel computer architectures together with suitably chosen algorithms [57]. In this spirit, we will in the following introduce and discuss parallelization strategies for Lanczos diagonalization and the TMM. These ideas have been implemented in a parallel CWI program (P-CWI) and a parallel TMM program (P-TMM) and used to generate the large system size data for Refs. [14,15,23–26,38,63–65].

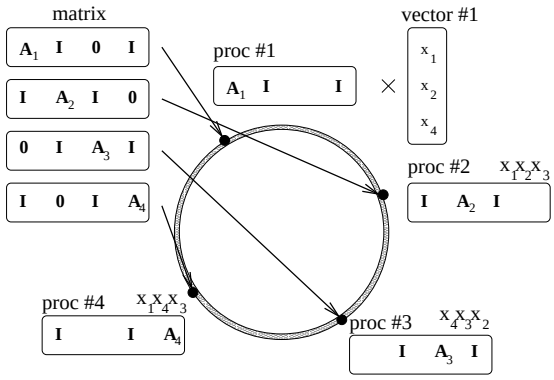


Fig. 2. Schematic diagram of the matrix-vector multiplication in the P-CWI for a $4^3$ system with periodic boundary conditions. The $16 \times 16$ matrices $\mathbf{A}_i$, $\mathbf{I}$, and $\mathbf{0}$ denote the Hamiltonian within the $i$th $4 \times 4$ plane and the coupling to the other planes. Each processor owns the part of the matrix and of the Lanczos vector corresponding to a single plane and the vectors of the two neighboring slices to which the matrix couples. Thus, processor #1 owns the slice vectors $x_1$, $x_2$, and $x_4$ (due to the periodic boundaries). In a ring topology network for the communication neighboring slices are located on neighbors in the ring.

### 4.1. *Parallel Lanczos diagonalization*

As reviewed in Sec. 3 the CWI is reliable and highly efficient for diagonalizing the Anderson Hamiltonian [5]. Therefore, it is worth trying to port it to parallel machines. Most of the computational effort in the Lanczos algorithm (at least in the case where only a few eigenvectors are to be computed) is spent on the iteration of Eq. (2), *i.e.*, on matrix-vector multiplications and vector additions. These can effectively be parallelized since in these operations each vector element can be calculated independently of all others. Thus, the main part of CWI is easily parallelized by splitting each of the Lanczos vectors $\mathbf{v}_i$ among the processors. This we call the distributed element scheme (DES). Each machine performs only part of the matrix-vector multiplication for each vector. All other parts of the code can be left more or less untouched. Here, a "naive parallelization" strategy is used: the eigenvectors to be computed are distributed over the nodes. In this manner, we implemented a parallel version of the CWI for distributed-memory architectures by using a parallelization library developed at the TU Chemnitz

[66].

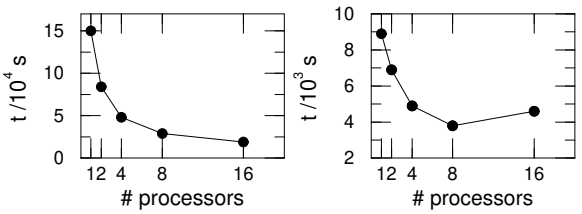


Fig. 3. Time to compute all eigenvalues (left) or 5 inner eigenvectors (right) using P-CWI for different numbers of processors on a Parsytec GC/Power Plus. The system size is $N^3 = 32^3$.

The parallel matrix-vector multiplication $\mathbf{Ax}$ is sketched in Fig. 2. We exploit the fact that a plane in the 3D cube couples only to the two neighboring planes. Each node owns the part of the matrix belonging to a number of adjacent slices of the cube and the corresponding part of the Lanczos vectors. Additionally, the vectors of the two neighboring slices are copied from the neighboring nodes and also stored locally. Now, each processor can perform its part of $\mathbf{Ax}$ independent of the others. This is implemented very efficiently with a number of nested loops; only the diagonal elements have to be stored.

Unfortunately, the resulting parallel Lanczos iteration does not scale very well, at least on the present hardware available at the TU Chemnitz. As can be seen in the right part of Fig. 3, the program needs more time on 16 processors than on 8. In each iteration step, the vectors of two planes have to be exchanged between neighboring processors, one forward and the other backward in the (virtual) ring network connecting the nodes. The time spent on this communication operation depends only on the system size, but it is independent of the number of processors in use. Furthermore, there are two inner products which require summations over all nodes. This takes more time if more processors are involved. Only the number of arithmetic operations scales nearly in an optimal way. But this needs only little time, since there are only 7 non-zero matrix elements per row in $\mathbf{A}$. For $N^3 = 32^3$, each of the 16 processors owns only two planes and almost all time is spent on communication. In order to run efficiently, each node must own a larger number of about $\mathcal{O}(10)$ slices.

In the case where all eigenvalues are to be computed, most of the time is spent on determining the eigenvalues of the tridiagonal matrix. In the P-CWI this part of the program is again "naively" parallelized. Each processor works on a different part of the energy interval of interest and one obtains nearly optimal speedup. Although the basic Lanczos iteration scales badly again, the overall performance is much better for larger numbers of processors compared to the eigenvector computation. In the left part of Fig. 3 it is shown that computing time still *decreases* from 8 to 16 processors for system size $N^3 = 32^3$. Most of the large-size data ($N^3 = 50^3$) used, *e.g.*, in Ref. [25] for energy level statistics were computed with P-CWI on a cluster of Linux PCs connected by Fast Ethernet.

We expect a thread parallelization [67] of the CWI for dual processor PCs to be quite efficient since no data have to be communicated over a network and the number of slices per processor is rather high. However, this was not yet tested due to the large changes in the program required.

### 4.2. *Parallel TMM*

The TMM algorithm mainly consists of two numerically expensive parts. First, there is the recursion Eq. (3) which is a matrix-vector multiplication. It can be parallelized as described in the previous section. Second, there is the reorthonormalization which needs most of the computing time ($\approx 90\%$) for larger system sizes.

For the matrix multiplication of the TMM there are at least two possibilities of parallelization. The first scheme is again the DES, *i.e.* based on storing the elements of each vector $\mathbf{x}_l$ on different machines as shown in Fig. 4. Thus the speedup of this part of the algorithm is proportional to the number of machines used. However, at the boundaries, the machines need to communicate due to the hopping in the direction perpendicular to the TMM propagation, *i.e.*, the $\mathbf{A}_l \cdot \mathbf{X}_l$ terms in Eq. (3). This decreases the speedup as in P-CWI. On the other hand, the reorthogonalization can be done fairly fast in this DES scheme since the relevant scalar products can be computed first locally and only a simple addition over all machines is needed. Thus

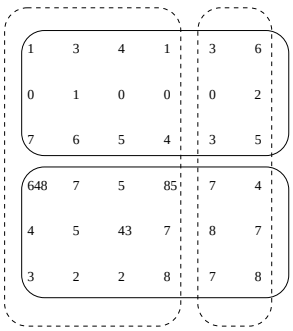


Fig. 4. Schematic diagram of the two possible schemes for storing vectors in the P-TMM. Each data column of the $6 \times 6$ matrix $\mathbf{X}$ represents a single vector. The solid lines indicate the distributed elements scheme (DES), whereas the dashed lines show the distributed vector scheme (DVS).

the DES decreases the amount of computer time needed for the matrix-vector multiplications and allows for a simple parallelization of the reorthogonalization.

The second parallelization scheme is based in storing the complete vectors on individual machines as also shown in Fig. 4. Let us call it the distributed vector scheme (DVS). No communication is needed for the matrix-vector multiplication part of the algorithm for the DVS and the speedup is proportional to the number of machines used. Unfortunately, the DVS needs a lot of communication for the reorthonormalization since it requires to send each vector to every other vector on each processor in order to compute the necessary scalar products. In Fig. 5 we show an implementation of the DVS scheme that is nevertheless rather effective for the orthogonalization.

At first glance, the second scheme looks much less convincing than the first, since in the reorthonormalization, machines such as `proc.#0` are idle for a long time. Nevertheless, a direct comparison between the distributed element (DES) and the distributed vector schemes (DVS) shows that the latter is faster. The DVS can be additionally accelerated by reducing the number of reorthonormalizations. This reduction can be achieved by adapting the number of matrix multiplications between successive reorthonormalizations according to the difference in norms of smallest and largest Lyapunov exponents [68,59] after each reorthonormalization. In Fig. 6 we show how these improvements lead to a reduction in the time needed for the P-TMM runs. For example, P-TMM runs for the 3D Anderson model with random hopping [12–15] with system size (cross section) $14 \times 14$ need only about 20% of computation time for 32 processors when compared to a single processor.

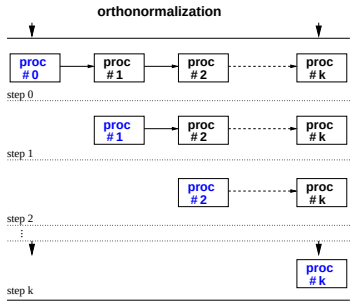


Fig. 5. Schematic diagram of the orthogonalization procedure for the P-TMM based on the DVS. The vectors in $\mathbf{X}_l$ are distributed on $k+1$ processors, so that the $i$th processor owns $n_i$ vectors. In step 0, the first of $n_0$ vectors on processor 0 is orthonormalized with respect to all other $n_0 - 1$ vectors and then sent to processor 1. Then the second vector on processor 0 is orthonormalized and so on until all $n_0$ vectors are orthonormal. In the meantime, the other processors have already orthonormalized their vectors with respect to the ones sent to them from processor 0. The algorithm now continues in step 1 with the $n_1$ vectors on processor 1 until finally in step $k$ all vectors on all $k$ machines are orthonormal.

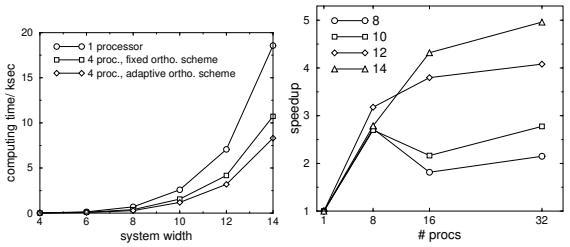


Fig. 6. Left: Performance data of the P-TMM for various implementations of the DVS algorithm. The times for data indicated by squares and diamonds in the left panel correspond to fixed and adaptive orthonormalization schemes as outlined in the text. Right: Speedup for different system sizes from $8 \times 8$ to $14 \times 14$ as a function of the number of processors used for the DVS. Note that the speedup for small system sizes decays upon increasing the number of processors already for a small number of processors due to the increased communication.

The speedup curves of Fig. 6 show that for the parallel architecture of a GC/PowerPlus-128 (Parsytec)-parallel computer (GCPP), the imple-

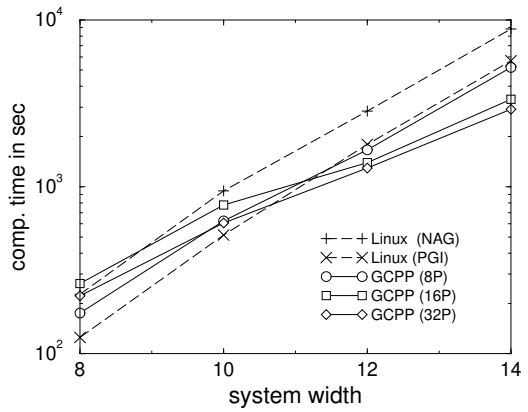


Fig. 7. Comparison of the best 3D P-TMM implementation on the GCPP with up to 32 processors with the 3D TMM implementation on a 400 MHz Pentium II (NAG, PGI) as a function of system size $M \times M$. NAG and PGI distinguish different Fortran compilers; the PGI compiler can optimize code for the Pentium II architecture.

mentation of the P-TMM does in fact give a net reduction in computing time for large system sizes. However, the real test of the usefulness of these codes comes when comparing to the performance on the fastest available serial computers. In Fig. 7 we show that at present due to the slowness of an individual processor on the GCPP, it is only for very large system sizes that the P-TMM performs better then its single-processor version on a Pentium II architecture.

We had hoped that a threaded parallelization would be very efficient on a shared-memory architecture dual processor PC. The inner loop of the reorthonormalization consists of an inner product and a vector multiplication/addition. The vectors are split in two parts and each CPU performs the operations for either the upper or lower half, independently of the other. Unfortunately, the gain was much less than expected, the speedup even for extreme system sizes of $M = 40$ was clearly less than 2. Two synchronizations are necessary to ensure that the correct result of the inner product is available on both processors. However, even for very large system sizes, in terms of the TMM, the vector lengths on the two nodes are only of the order of $M^2 = 30^2 = 900$. Since the vector operations are performed extremely efficiently by using a machine specific optimized BLAS library [69], the effort of the synchronization is apparently not small compared to the $\mathcal{O}(900)$ floating point operations.

An equivalent parallelization of the Lanczos iteration can be expected to be much more efficient. Although there are two global summations and thus 4 synchronizations instead of 2 in each iteration step, the vector lengths would be of the order $N^3 = 50^3 = 125000$ resulting in a better arithmetic-to-communication ratio.

## 5. Conclusions

In conclusion, we have considered the strategies employed in our parallelization schemes for the CWI and the TMM in the Anderson model of localization. Both algorithms rely on fast matrix-vector multiplications and this part of the algorithms is ideally suited for a massively parallel approach. On the other hand, the efficiency of P-CWI is reduced due to the increasing communication between different sections of the matrix. Also, the efficiency of P-TMM is limited due to the required orthogonalization of all vectors with each other which necessarily implies a large communication effort.

Our results show that the application of parallel methods to the Anderson problem is nevertheless useful when large system sizes have to be reached, *e.g.* for a special set of parameters such as $E = 0$ and $W_c = 16.5$ that characterize the MIT. There, we have been able to investigate hitherto unreached system sizes.

*Acknowledgments*

This work was supported by the Deutsche Forschungsgemeinschaft within the Sonderforschungsbereich 393 "Numerische Simulation auf massiv parallelen Rechnern".

## References

[1] P. A. Lee, T. V. Ramakrishnan, Disordered electronic systems, Rev. Mod. Phys. 57 (1985) 287–337.

[2] B. Kramer, A. MacKinnon, Localization: theory and experiment, Rep. Prog. Phys. 56 (1993) 1469–1564.

[3] D. Belitz, T. R. Kirkpatrick, The Anderson-Mott transition, Rev. Mod. Phys. 66 (1994) 261–380.

[4] P. W. Anderson, Absence of diffusion in certain random lattices, Phys. Rev. 109 (1958) 1492–1505.

[5] U. Elsner, V. Mehrmann, F. Milde, R. A. Römer, M. Schreiber, The Anderson model of localization: a challenge for modern eigenvalue methods, SIAM J. Sci. Comp. 20 (1999) 2089–2102, ArXiv: physics/9802009.

[6] P. Häussler, Interrelations between atomic and electronic structures — liquid and amorphous metals as model systems, Phys. Rep. 222 (1992) 65–143.

[7] N. F. Mott, H. Jones, The Theory of the Properties of Metals and Alloys, Dover Publications, New York, 1958.

[8] A. Möbius, C. J. Adkins, Metal-insulator transition in amorphous alloys Preprint.

[9] M. A. Paalanen, G. A. Thomas, Experimental tests of localization in semiconductors (metal-insulator transition), Helv. Phys. Acta 56 (1983) 27–34.

[10] G. A. Thomas, in: D. M. Finlayson (Ed.), Localisation and Interactions in Disordered and Doped Semiconductors, SUSSP, Edinburgh, 1986, p. 172.

[11] B. Kramer, M. Schreiber, Transfer-matrix methods and finite-size scaling for disordered systems, in: K. H. Hoffmann, M. Schreiber (Eds.), Computational Physics, Springer, Berlin, 1996, pp. 166–188.

[12] A. Eilmes, R. A. Römer, M. Schreiber, The two-dimensional Anderson model of localization with random hopping, Eur. Phys. J. B 1 (1998) 29–38.

[13] A. Eilmes, R. A. Römer, M. Schreiber, Critical behavior in the two-dimensional Anderson model of localization with random hopping, phys. stat. sol. (b) 205 (1998) 229–232.

[14] P. Cain, Das Anderson-Modell der Lokalisierung mit nichtdiagonaler Unordnung, Master's thesis, Technische Universität Chemnitz (December 1998).

[15] P. Biswas, P. Cain, R. A. Römer, M. Schreiber, Off-diagonal disorder in the Anderson model of localization, phys. stat. sol. (b) 218 (2000) 205–209, ArXiv: cond-mat/0001315.

[16] B. Bulka, M. Schreiber, B. Kramer, Localization, quantum interference, and the metal-insulator transition, Z. Phys. B 66 (1987) 21.

[17] T. Brandes, B. Huckestein, L. Schweitzer, Critical dynamics and multifractal exponents at the Anderson transition in 3d disordered systems, Ann. Phys. (Leipzig) 5 (1996) 633–651.

[18] A. Eilmes, U. Grimm, R. A. Römer, M. Schreiber, Two interacting particles at the metal-insulator transition, Eur. Phys. J. B 8 (1999) 547–554.

[19] M. Schreiber, Multifractal characteristics of electronic wave functions in disordered systems, in: K. H. Hoffmann, M. Schreiber (Eds.), Computational Physics, Springer, Berlin, 1996, pp. 147–165.

[20] G. H. Golub, C. F. v. Loan, Matrix Computations, 3rd Edition, Johns Hopkins University Press, Baltimore and London, 1996.

[21] Q. Li, C. M. Soukoulis, E. N. Economou, G. S. Grest, Anisotropic tight-binding model for localization, Phys. Rev. B 40 (1989) 2825–2830.

[22] Q. Li, S. Katsoprinakis, E. N. Economou, C. M. Soukoulis, Scaling properties in highly anisotropic systems, Phys. Rev. B 56 (1997) R4297–R4300, ArXiv: cond-mat/9704104.

[23] F. Milde, R. A. Römer, M. Schreiber, Multifractal analysis of the metal-insulator transition in anisotropic systems, Phys. Rev. B 55 (1997) 9463–9469.

[24] F. Milde, R. A. Römer, Energy level statistics at the metal-insulator transition in the Anderson model of localization with anisotropic hopping, Ann. Phys. (Leipzig) 7 (1998) 452–456.

[25] F. Milde, R. A. Römer, M. Schreiber, Energy level statistics at the metal-insulator transition in anisotropic systems, Phys. Rev. B 61 (2000) 6028–6035, ArXiv: cond-mat/9909210.

[26] F. Milde, R. A. Römer, M. Schreiber, V. Uski, Critical properties of the metal-insulator transition in anisotropic systems, Eur. Phys. J. B 15 (2000) 685–690, ArXiv: cond-mat/9911029.

[27] M. Schreiber, H. Grussbach, Multifractal wave functions at the Anderson transition, Phys. Rev. Lett. 67 (1991) 607–610.

[28] E. Hofstetter, Critical behavior at the metal-insulator transition in three-dimensional disordered systems in a strong magnetic field, Phys. Rev. B 54 (1996) 4552–4557, ArXiv: cond-mat/9604100.

[29] T. Kawarabayashi, B. Kramer, T. Ohtsuki, Numerical study on Anderson transitions in three-dimensional disordered systems in random magnetic fields, Ann. Phys. (Leipzig) 8 (1999) 487–496, ArXiv: cond-mat/9907319.

[30] T. Kawarabayashi, B. Kramer, T. Ohtsuki, Anderson transition in three-dimensional disordered systems with randomly varying magnetic flux, Phys. Rev. B 57 (1998) 11842–11845, ArXiv: cond-mat/9803192.

[31] D. K. K. Lee, J. T. Chalker, D. Y. K. Ko, Localization in a random magnetic field: The semiclassical limit, Phys. Rev. B 50 (1994) 5272–5285.

[32] X. R. Wang, C. Y. Wong, X. C. Xie, Metal-insulator transition in a multilayer system with a strong magnetic field ArXiv: cond-mat/9904358.

[33] D. K. K. Lee, J. T. Chalker, Unified model for two localization problems: Electron states in spin-degenerate landau levels and in a random magnetic field, Phys. Rev. Lett. 72 (1994) 1510–1513.

[34] S. Chakravarty, S. Kivelson, C. Nayak, K. Völker, Wigner glass, spin-liquids, and the metal-insulator transition ArXiv: cond-mat/9805383.

[35] T. Okamoto, K. Hosoya, S. Kawaji, A. Yagi, A. Yutani, Y. Shiraki, Metal-insulator transition and spin degree of freedom in silicon 2D electron systems ArXiv: cond-mat/9906425.

[36] E. Abrahams, P. W. Anderson, D. C. Licciardello, T. V. Ramakrishnan, Scaling theory of localization: absence of quantum diffusion in two dimensions, Phys. Rev. Lett. 42 (1979) 673–676.

[37] T. Ando, J. Phys. Soc. Japan 53 (1984) 3126.

[38] M. Schreiber, F. Milde, R. A. Römer, U. Elsner, V. Mehrmann, Electronic states in the Anderson model of localization: benchmarking eigenvalue algorithms, Comp. Phys. Comm. 121–122 (1–3) (1999) 517–523.

[39] S. N. Evangelou, E. N. Economou, Spectral density singularities, level statistics, and localization in a sparse random matrix ensemble, Phys. Rev. Lett. 68 (1992) 361–364.

[40] B. I. Shklovskii, B. Shapiro, B. R. Sears, P. Lambrianides, H. B. Shore, Statistics of spectra of disordered systems near the metal-insulator transition, Phys. Rev. B 47 (1993) 11487–11490.

[41] E. Hofstetter, M. Schreiber, Statistical properties of the eigenvalue spectrum of the three-dimensional Anderson Hamiltonian, Phys. Rev. B 48 (1993) 16979–16985.

[42] M. Janssen, Statistics and scaling in disordered mesoscopic electron systems ArXiv: cond-mat/9703196.

[43] M. Batsch, L. Schweitzer, I. K. Zharekeshev, B. Kramer, Crossover from critical orthogonal to critical unitary statistics at the Anderson transition, Phys. Rev. Lett. 77 (1996) 1552–1555, ArXiv: cond-mat/9607070.

[44] M. Batsch, Numerical studies on level statistics of electrons in disordered systems, Ph.D. thesis, Universität Hamburg (1997).

[45] A. D. Mirlin, Y. V. Fyodorov, The statistics of eigenvector components of random band matrices: analytical results, J. Phys. A: Math. Gen. 26 (1993) L551–L558.

[46] V. Fal'ko, K. B. Efetov, Statistics of fluctuations of wave functions of chaotic electrons in a quantum dot in an arbitrary magnetig field, Phys. Rev. B 50 (1994) 11267–11270.

[47] V. I. Fal'ko, K. B. Efetov, Statistics of prelocalized staes in disordered conductors, Phys. Rev. B 52 (1995) 17413–17429.

[48] K. Müller, B. Mehlig, F. Milde, M. Schreiber, Statistics of wave functions in disordered and in classically chaotic systems, Phys. Rev. Lett. 78 (1997) 215–218.

[49] V. Uski, B. Mehlig, R. A. Römer, A numerical study of wave-function and matrix-element statistics in the Anderson model of localization, Ann. Phys. (Leipzig) 7 (1998) 437–441.

[50] R. A. R. V. Uski, B. Mehlig, M. Schreiber, An exact diagonalization study of rare events in disordered conductors, Phys. Rev. B in press.

[51] J. Cullum, R. A. Willoughby, Lanczos Algorithms for Large Symmetric Eigenvalue Computations, Volume 1: Theory, Birkhäuser, Boston, 1985.

[52] J. Cullum, R. A. Willoughby, Lanczos Algorithms for Large Symmetric Eigenvalue Computations, Volume 2: Programs, Birkhäuser, Boston, 1985, `http://www.netlib.org/lanczos/`.

[53] R. B. Lehoucq, J. A. Scott, An evaluation of software for computing eigenvalues of sparse nonsymmetric matrices, Tech. Rep. MCS-P547-1195, Argonne National Laboratory, Argonne, `ftp://info.mcs.anl.gov/pub/tech_reports/reports/P547.ps.Z` (1996).

[54] R. B. Lehoucq, D. Sorensen, C. Yang, ARPACK users guide: Solution of large scale eigenvalue problems by implicitly restarted Arnoldi methods, Tech. rep., Rice University, Department of Computational and Applied Mathematics, Houston, `http://www.caam.rice.edu/software/ARPACK/ug.ps` (1996).

[55] D. Sorensen, C. Sun, private communications.

[56] R. Barrett, M. Berry, T. Chan, J. Demmel, J. Donato, J. Dongarra, V. Eijkhout, R. Pozo, C. Romine, H. A. v. d. Vorst, Templates for the solution of linear systems, SIAM Publications, Philadelphia, 1994.

[57] F. Milde, Disorder-induced metal-insulator transition in anisotropic systems Dissertationsschrift, Technische Universität Chemnitz.

[58] A. MacKinnon, B. Kramer, One-parameter scaling of localization length and conductance in disordered systems, Phys. Rev. Lett. 47 (1981) 1546–1549.

[59] A. MacKinnon, B. Kramer, The scaling theory of electrons in disordered solids: additional numerical results, Z. Phys. B 53 (1983) 1–13.

[60] J.-L. Pichard, G. Sarma, Finite-size scaling approach to Anderson localisation, J. Phys. C 14 (1981) L127–L132.

[61] J.-L. Pichard, G. Sarma, Finite-size scaling approach to Anderson localisation: II. quantitative analysis and new results, J. Phys. C 14 (1981) L617–L625.

[62] R. A. Horn, C. R. Johnson, Matrix Analysis, Cambridge University Press, New York, 1985.

[63] R. A. Römer, M. Schreiber, No enhancement of the localization length for two interacting particles in a random potential, Phys. Rev. Lett. 78 (1997) 515–518.

[64] P. Cain, R. A. Römer, M. Schreiber, Phase diagram of the three-dimensional Anderson model of localization with random hopping, Ann. Phys. (Leipzig) 8 (1999) SI33–SI38, ArXiv: cond-mat/9908255.

[65] R. A. Römer, From localization to delocalization in disordered systems Habilitationsschrift, Technische Universität Chemnitz.

[66] G. Haase, T. Hommel, A. Meyer, M. Pester, Bibliotheken zur Entwicklung paralleler Algorithmen, Tech. Rep. SPC 95_20, TU Chemnitz, `http://www.tu-chemnitz.de/sfb393/spc95pr.html` (Jun. 1995).

[67] WWW-reference, Online reference for threads, `http://pauillac.inria.fr/~xleroy/linuxthreads/`; `http://www.serpentine.com/~bos/threads-faq/`, likely to change without prior notice (1999).

[68] O. Halfpap, Interaction induced delocalization of electrons in disordered systems?, Master's thesis, Universität Hamburg (December 1996).

[69] WWW-reference, `http://www.cs.utk.edu/~ghenry/distrib/index.htm`, likely to change without prior notice (1999).